

MMSE Adaptive Receiver vs. Rake Receiver Performance Evaluation for UWB Signals over Multipath Fading Channel

Nadir Mohamed Abd Elaziz

Jazan University – CNET Dept. – Deanship of Community Service and Continuing Education

Abstract: - this paper presents a performance comparison between Minimum-Mean-Square-Error (MMSE) adaptive receiver as a reception algorithm utilizing a new specific template Ultra-wideband (UWB) pulse shape, and the performance of conventional Ultra-Wideband (UWB) Rake receiver with different number of Rake fingers. MMSE adaptive algorithm is more efficient and powerful because of its ability and features of adaptation to the substantial changes in the UWB multipath wireless communication channel model proposed by the IEEE 802.15.3a working group based on modified (S-V) channel model; employing two commonly used transmission and multiple access schemes in UWB communications which are Direct-Sequence (DS-UWB) and Time-Hopping (TH-UWB). Moreover, the performance comparison between the two reception schemes presented in this paper is assumed to be performed in the presence of both; narrowband interference coming from other networks (e.g. IEEE 802.11a WLAN), and also the presence of Multiple-Access-Interference (MAI) coming from other UWB users in the proximity of the desired UWB user.

Key Words: - Ultra-Wideband (UWB), Multiple-Access-Interference (MAI), Federal-Communication-Committee (FCC), Bit-Error-Rate (BER), Signal-to-Noise Ratio (SNR), Signal-to-Interference-Noise Ratio (SINR), Power-Spectral-Density (PSD), Minimum-Mean-Square-Error (MMSE), Channel-Model (CM).

I. INTRODUCTION

The field of UWB has drawn a lot of attention and study effort in the last few years as it seems to be a better candidate compared to most of the existing wireless radio technologies supporting short-range high-speed (high data rates) communication networks. A substantial change occurred in February 2002; when the Federal Communication Committee (FCC) has issued ruling report states that UWB signals with its associated very wide bandwidth (7.5 GHz), and extremely low power-spectral-density (PSD) up to -41.3 dBm could be used for commercial data communication applications such as wireless Personal Area Networks (WPANs), the FCC regulation report defines the UWB signal as “ a signal that has a – 10dB bandwidth spectrum greater than at least 500 MHz, or a signal that has a fractional bandwidth (F_{BW}) greater than or equal to 0.20” [1], the fractional bandwidth is defined by the following equation; whereas f_c represents the central frequency, f_H and f_L correspond to the high and low frequencies identifying the – 10dB bandwidth respectively [1].

$$F_{BW} = \frac{f_H - f_L}{f_c} = 2 \cdot \frac{f_H - f_L}{f_H + f_L} \geq 0.20 \quad \dots\dots\dots (1)$$

Furthermore, UWB became an emerging solution for the IEEE 802.15a (TG3a) standard; which is to provide a low complexity, low cost, low power consumption and high data rates among WPANs devices. UWB systems are considered more preferable due to the simple design of the transceiver structure resulting from the fact that; UWB signals are “carrier less” (transmitted without any carrier sinusoidal wave); the feature that eliminates the need for modulator, demodulator, and oscillators circuitries in the transceiver structure. UWB communications utilizes extremely narrow pulses to convey the carrier less UWB signals over the inherited wide spectrum bandwidth [1] [2]. However, the system model is introduced in section II which characterizes the UWB pulse shapes used in the paper and the proposed UWB multipath channel models. While the transmission and multiple access schemes are presented in section III. Section IV demonstrates in details the block diagrams and theory of operation of the different reception schemes and receiver structures. The simulation and performance comparison results are illustrated using MATLAB R2013b and Simulink libraries in section V. Finally, section VI concludes the finishing results of the performance evaluation for the different receiver structures discussed in the paper.

II. SYSTEM MODEL

A. UWB Pulse Shape

Since FCC issued a ruling report in February 2002 authorizing that UWB technology is considered an interesting candidate for indoor wireless communications in the spectrum domain 3.1 – 10.6 GHz for its ability to convey information with very high data rates inherited from the ultra-wide bandwidth (7.5 GHz). UWB utilizes extremely narrow pulses (sub-nanosecond) to spread its signal’s power over the wide bandwidth, taking to consideration that these extremely narrow pulses must fulfill the FCC power spectral density (PSD) requirements presented in the ruling report as “UWB systems indoor spectral Mask limits” shown in Fig. 1.

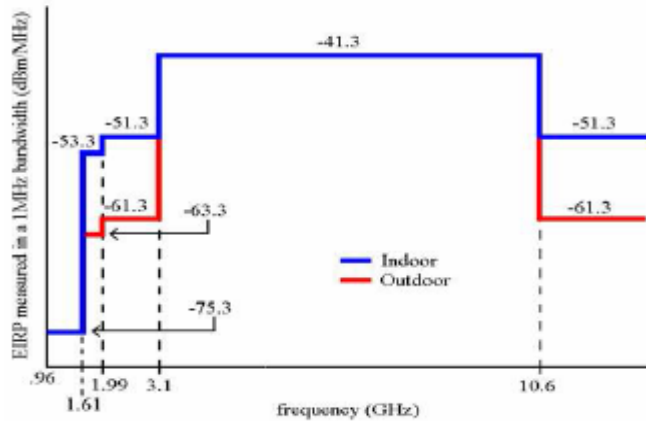


Fig. 1: UWB indoor Radiated power mask regulated by FCC

The narrow UWB pulses are emitted from the transmitter in a unique rhythm called “Pulse Repetition Rate” associated to each transmitter and it must be known at the receiver to be able to detect the data and information signal being transmitted. One fundamental challenge is to maximize the radiated UWB pulse energy; yet to assure that the pulse’s PSD complies with the FCC spectral mask limits. Moreover, since the extremely narrow pulses are relatively easy to generate with analog components; the Gaussian “monocycle” pulse and its derivatives are commonly used as basic UWB pulse shapes because their PSD comply with the FCC mask power limits as demonstrated in Fig. 2 [3] [4]. Hence, the pulse shapes used in the simulation in the paper are the derivatives of the Gaussian “monocycle” pulse which can be expressed in the following equation:

$$y_{Gn}(t) = \frac{d^n}{dt^n} \left(A \cdot \exp\left(-\frac{t}{\eta}\right)^2 \right) \dots\dots\dots (2)$$

Where; A is the normalized Pulse amplitude, and η is a time-scaling factor and its relation to the pulse width T_p is that $T_p = 7\eta$ which contains about 99.98% of the total pulse energy.

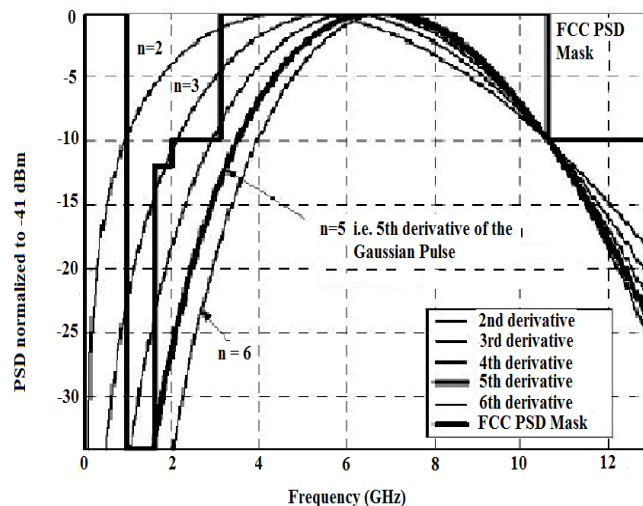


Fig. 2: PSDs of higher order derivatives of UWB Gaussian pulses

It can be seen from Fig. (2) that; PSD of the first derivative of the *Gaussian “monocycle” pulse* does not totally fit within the FCC spectral mask. Therefore, another pulse shapes founded from derivatives of the *Gaussian Pulse* because the higher-order derivatives increases the number of zero crossings which correspond to higher “carrier” frequency sinusoid modulated by an equivalent Gaussian envelope. Thus, the *Gaussian Doublet* which is the 2nd derivative of the *Gaussian Pulse* expressed in (3) is the most commonly used UWB pulse shape in the literature [4]. However, this paper studies and analyzes the performance of the 6th derivative of the *Gaussian Pulse* represented in (4) since it satisfies more the power limits of the FCC report and fits much better into the mask limits as shown in Fig. (2).

$$y_{G_2}(t) = \left(1 - 4\pi \left(\frac{t}{\eta}\right)^2 \right) \cdot \exp \left(- 2\pi \left(\frac{t}{\eta}\right)^2 \right) \dots\dots\dots (3)$$

$$y_{G_6}(t) = \left(1 - 12\pi \cdot \left(\frac{t}{\eta}\right)^2 + 16\pi^2 \cdot \left(\frac{t}{\eta}\right)^4 - \frac{64}{15}\pi^3 \cdot \left(\frac{t}{\eta}\right)^6 \right) \cdot \exp \left(- 2\pi \cdot \left(\frac{t}{\eta}\right)^2 \right) \dots\dots\dots (4)$$

B. UWB Multipath Channel Model

The modified Saleh-Valenzuela (S-V) model is used in the paper since it was adopted as a reference UWB channel model by the IEEE 802.15.3a working group. The modeling process is based on an indoor propagation environment practical measurement, and the main distinct features of the UWB propagation channel are; the extremely rich multipath components profile and the non-Rayleigh fading amplitude characteristics. In UWB propagation there are much more multipath components than any other wireless propagation channels. As a result of the wide bandwidth of UWB pulses’ waveforms; the different objects exist in the indoor environment will give a rise to much several multipath components all of which would be a part of one “cluster”. Thus, the multipath components arrive at the receiver end in the form of “clusters”, and within each cluster there will be multiple subsequent arrivals called “rays”. Therefore, Time-Of-Arrival (TOA) statistics the IEEE 802.15.3a standard model used (S-V) approach which modeled multipath components in clusters and rays. Since UWB pulses are extremely narrow; only few multipath components overlap within each resolvable delay bin. Consequently; the central limit theorem is not applicable and the amplitude fading statistics are not sufficiently represented by Rayleigh distribution. The IEEE 802.15.3a standard adopted the modified (S-V) model because its amplitude fading statistics are Log-normally distributed [4]. The impulse response of the modified (S-V) model is represented in equation (5) [2] [4]:

$$h_i(t) = X_i \sum_{l=0}^{L_c-1} \sum_{k=0}^{K_{lc}-1} \alpha_{k,l} \cdot \delta(t - T_l^i - \tau_{k,l}^i) \dots\dots\dots(5)$$

Where; $\alpha_{k,l}^i$ represents the multipath gain coefficients, T_l^i represents the delays of the l th cluster, $\tau_{k,l}^i$ represents the delays of the k th multipath component “ray” within the l th cluster arrival time (T_l^i). Shadowing effect of the total multipath energy is log-normal distributed and is represented by the term X_i , and i refers to the i th realization.

A calculation of the delay characteristics of the modified (S-V) model impulse response presented in (5) simulated using MATLAB and the simulation results are shown in Fig. 3. as can be seen in the figure; for any longer delay in time-domain the amplitudes of UWB signal’s pulses are more decreasing and reduced; which is expressed as “Fading” due to the multipath delay spread of the different rays within each of the different clusters.

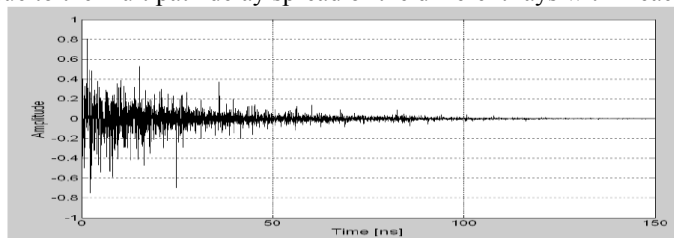


Fig. 3: Impulse Response and Delay Profile of Modified Saleh-Valenzuela Model

The IEEE 802.15.3a standard multipath channel proposal has defined four different models for different scenarios based on practical measurements found in the indoor environment which are characterized as:

- CM1: Line-Of-Sight (LOS) model for distance 0 – 4 m between T_x and R_x .

- CM2: Non-LOS (NLOS) model for distance 0 – 4 m between T_x and R_x .
- CM3: NLOS model for distance 4 – 10 m between T_x and R_x .
- CM4: NLOS for 4 – 10 m between T_x and R_x , with extreme (dense) multipath channel condition.

III. TRANSMISSION AND MULTIPLE ACCESS

As mentioned in the previous section the UWB pulses must be transmitted as a train of pulses in a rhythm or a regular time called “pulse repetition rate” to carry the information signal for short range (indoor environment). However, this regular pulse repetition rate will cause relatively large frequency PSD peaks of amplitude in the corresponding spectrum at a certain frequencies represent the inverse of the pulse repetition rate as presented in Fig. 4.a and 4.b respectively which contradicts and breaches the FCC power mask regulations. However, one approach to avoid the regular periodic transmission of UWB pulses is to “dither” the transmitted UWB pulse train by adding a small random offset to each pulse, either delaying the pulse or transmitting slightly before its regular time. The resultant spectrum from such a random offset is shown in Fig. 5; which presents an observable reduction in the PSD amplitude peaks compared to Fig. 4.b [3].

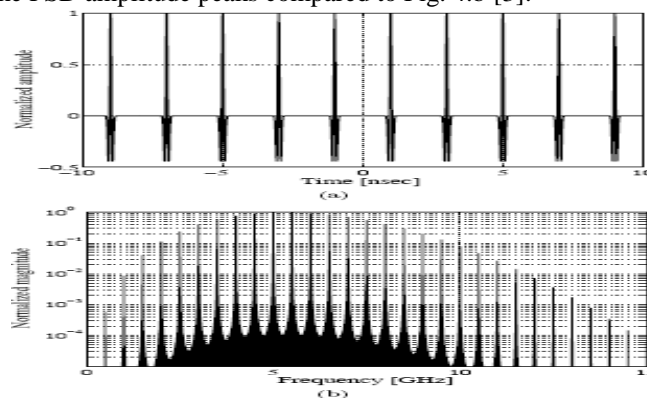


Fig. 4: (a) UWB pulse train. (b) Frequency spectrum of UWB pulse train.

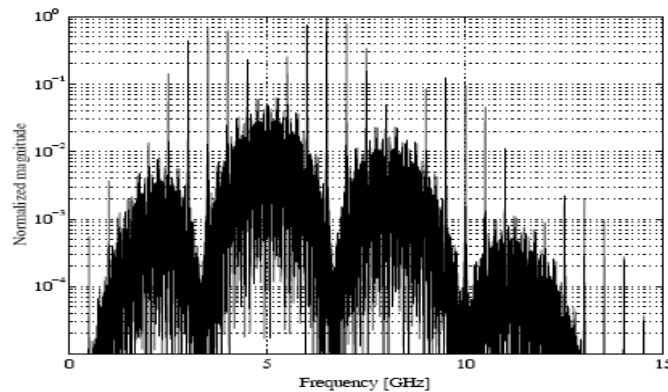


Fig. 5: Spectrum of the dithered UWB pulse train

Furthermore, the same approach besides dithering the UWB signal periodic pulse train and reducing the PSD amplitude peaks, it also can be used as a “multiple access” scheme for distinguishing each different UWB User by its own random offset. There are two randomizing techniques “multiple access” schemes can be employed to achieve the required goals which are; Direct-Sequence UWB (DS-UWB), and Time-Hopping UWB (TH-UWB). In DS-UWB the Bandwidth spreading effect is achieved by the UWB pulse shaping. The basic format of the DS-UWB for the k th impulse radio transmitter (user) output signal $S_{ir}^{(k)}(t)$ is given by equation (6) [4]:

$$s_{ir}^{(k)}(t) = \sqrt{P_k} \sum_{j=-\infty}^{\infty} \sum_{n=0}^{N_c-1} b_j^{(k)} \cdot c_n^{(k)} \cdot w_{ir}(t - jT_f - nT_c) \dots (6)$$

Where; $w_{ir}(t)$ represents the transmitted UWB pulse monocycle, $c_n^{(k)}$ denotes the PN sequence associated to

the k th user, T_f is the symbol (frame) period, T_c is the chip period such that $T_f = N_c \cdot T_c \cdot b_j^{(k)}$ represents the information bit stream of the k th user, P^k is the transmitted power corresponding to the k th user. n is an integer = 0,1,2,..., $c_n^{(k)}$ represents the PN sequence associated to the k th user, $b_j^{(k)} \in \left\{ \begin{matrix} + \\ 1 \\ - \end{matrix} \right\}$ is the BPSK data

(bit) stream of the k th user, T_f is the pulse repetition period (frame time), T_c is the chip period. While Time-Hopping UWB usually utilizes Pulse-Position-Modulation (PPM) as a modulation scheme. In UWB systems the pulses are assumed to be one of desired UWB pulse shapes mentioned in the previous sub-section. The basic format of the TH using PPM for the k th user transmitted signal is given by [4]:

$$s_{ir}^{(k)}(t) = \sum_{j=-\infty}^{\infty} w_{ir}(t - jT_f - c_j^{(k)}T_c - b_j^{(k)}T_{PPM}) \dots \quad (7)$$

Where; $c_j^{(k)}$ represents the PN Time-Hopping sequence associated to the k th user, T_{PPM} represents the pulse time-shift for the Pulse-Position-Modulation (PPM). The time-shift element of the TH code word assigned to the k th user is chosen from the set: $j = 0, 1, 2 \dots N_c - 1$; Where N_c is the number of time-delay bins (chips) in a frame time T_f .

IV. RECEPTION SCHEMES AND STRUCTURES

The extremely narrow pulses used in UWB systems give a rise to the phenomena of *Multipath* characterized by the UWB wireless channel discussed previously in section II due to the mechanisms of reflection, diffraction, and scattering which cause the transmitted UWB signal to be; diverted into many paths, and its energy to be dispersed, and also to arrive at the receiver end after some delays according to each path length and losses. UWB systems utilize spread spectrum techniques as (DS) and (TH) mentioned in section III; the thing that require great accuracy in signal acquisition, synchronization, and tracking at the receiver end.

C. UWB Rake receiver

The previously mentioned UWB multipath channel conditions cause significant signal degradations, and consequently make it essential to solve the dispersed signal energy problem and capture as much energy as possible to reconstruct the heavily degraded UWB signal. Rake receiver is a single-user detector designed to collect as much energy as possible from the signal's multipath components and then combine their contributions together to estimate the transmitted symbol [3]. The UWB Rake receiver extracts information modulated on the UWB Gaussian pulse from the degraded and distorted received waveforms with high accuracy utilizing "correlators" as seen in Fig. 6. Moreover, Rake receiver attempts to collect the time-shifted versions of the original UWB signal by providing a separate correlation receiver for each of the multipath components; each of the correlator receivers is adjusted in time delay so that it can search in different time windows called "search window" for significant multipath components. Rake receiver utilizes multiple correlators to separately detect the strongest multipath components; and then the outputs of the correlators are weighted to provide a better estimate of the transmitted UWB signal than is provided by a single component.

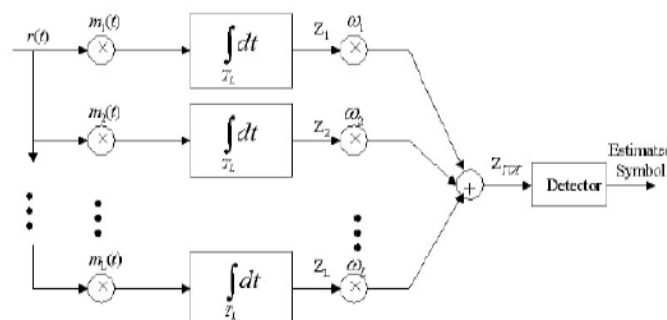


Fig. 6: UWB Rake receiver Block diagram

The term "All Rake" (A-Rake) is used in the literature to indicate the Rake receiver with unlimited resources that utilizes all the multipath components or correlator taps as shown in Fig. 7. Therefore, this type of Rake receiver

is considered efficient from the energy capture perspective; yet, it is considered inefficient from the circuit implementation and complexity point of view. Another structure of UWB Rake receiver is the “Selective Rake” (S-Rake) which selects and combines the “M” best multipath components or taps out of the total “L” multipath components that is determined by the Rake finger selection algorithm as presented in Fig. 8 [4] [5].

Furthermore, the “Partial combining Rake” receiver structure (P-Rake) uses “N” multipath components out of the total “L” available diversity multipath; but it combines the first “N” arriving components which are not necessarily the strongest nor the best. The P-Rake structure has drastically reduced the complexity compared to the S-Rake structure due to the absence of the selection mechanism. Thus, the P-Rake mitigates the need to sort the multipath components by their instantaneous path gain magnitudes which would require a highly accurate channel estimation process.

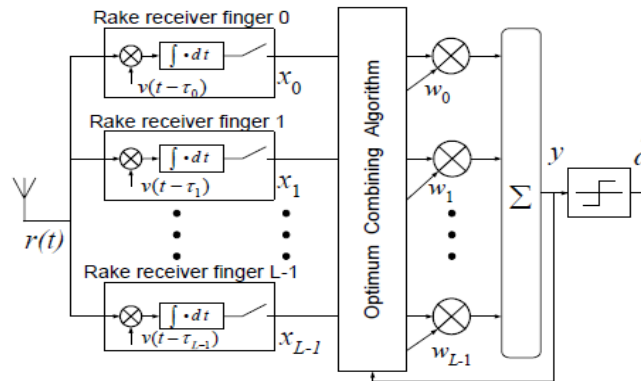


Fig. 7: “All Rake” receiver Block diagram

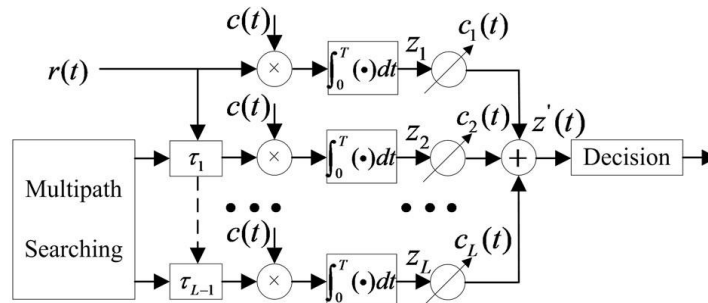


Fig. 8: “Selective Rake” receiver Block diagram

Instead, the P-Rake structure only needs to find the “position” of the first arriving multipath component, which leads to a substantial circuit complexity reduction.

D. Minimum Mean Square Error (MMSE) algorithm

Significant studies have been made on an adaptive correlator receiver by Pateros and Saulnier in the field of “Direct-Sequence Spread Spectrum” (DS-SS) systems employing BPSK signaling in a single user, time-invariant multipath environment; these studies have proven that MMSE algorithm receiver detects the transmitted data, removes the interference, and coherently combines the multipath components of the signal in the presence of Narrowband Interference (NBI). However, this paper demonstrates the performance of the MMSE correlator receiver with its adaptive algorithm and capabilities for both DS-UWB and TH-UWB transmission schemes discussed previously in section III. A major advantage of the MMSE scheme relative to other interference suppression reception schemes is that; explicit knowledge of the interference parameters is not required. Instead, the UWB received signal (template 6th derivative Gaussian pulses) from the multipath components can be sampled at a rate equal to the Pulse-Repetition-Frequency after passing through the correlator receivers with their path selection mechanism, and then the samples are linearly combined using the MMSE algorithm criteria to suppress the NBI and consequently maximize the SINR as shown in Fig. 9.

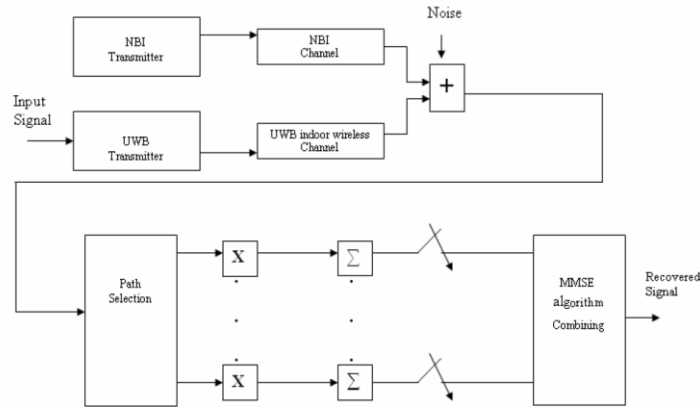


Fig. 9: UWB MMSE receiver Scheme

Moreover, the MMSE adaptive algorithm receiver consists of two parts; First, correlator receivers which combines the contribution of the strongest best multipath components and mitigates the effect of noise to maximize the SNR. Second, the adaptive filter which is mainly a Finite-Impulse-Response (FIR) digital filter that essentially acts as a matched filter to correlate the received UWB pulse waveform with the well-known template waveform and then re-adjusts the correlator receiver’s taps weights to minimize the Mean Square Error using an adaptive algorithm despite the type of noise and interference may be present in order to maximize the SINR as demonstrated precisely in Fig. 10 [6].

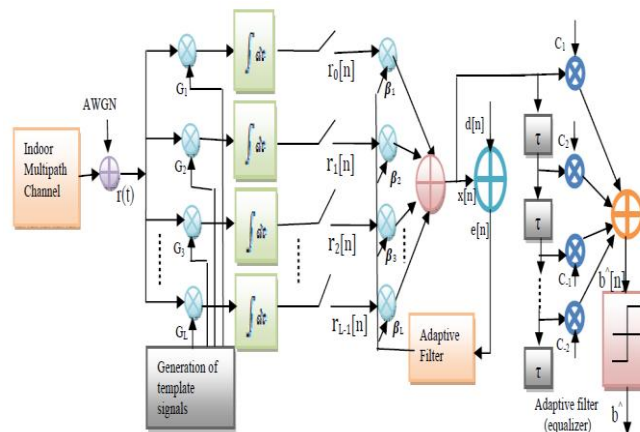


Fig. 10: MMSE Adaptive Algorithm receiver Block diagram

Adaptive algorithms such as “Recursive Least Squares” (RLS) adaptive filter is an algorithm which recursively finds the filter coefficients that minimize a weighted linear least squares cost function relating to the input signals. This is in contrast to other adaptive algorithms such as “Least Mean Squares” (LMS) that aim to reduce the mean square error. In the derivation of the RLS in [5], the input signals are considered deterministic, while for the LMS and similar algorithm they are considered stochastic. Compared to most of its competitors, the RLS exhibits extremely fast convergence. However, this benefit comes at the cost of high computational complexity [5].

V. SIMULATION AND RESULTS

The paper presents performance evaluation of two different transmissions multiple access techniques over UWB multipath NLOS channel employing two different receiver structures and schemes on BER vs. SNR basis, assuming the utilized UWB template pulse shape to be the 6th derivative Gaussian pulse demonstrated in equation (4). The simulation results are obtained by MATLAB codes and SIMULINK library blocks and communication tools for; the performance comparison between DS-UWB and TH-UWB using BPM and PPM modulation techniques respectively, in the presence of AWGN along with NBI presumed to be coming from IEEE 802.11a WLAN source over UWB multipath NLOS channel based on the modified (S-V) channel model CM3. Moreover, the simulations present another important performance comparison between two significant receiver structures schemes; First, Rake receiver with finger selection mechanism and different number of fingers (4 fingers, 8 fingers, and 128 or an infinite “∞” number of fingers). Second, Minimum Mean Square

Error (MMSE) correlator receiver with LMS, RLS adaptive algorithms to re-adjust the tap weights for noise and interference suppression to maximize the SINR. The rest of the key simulation parameters are listed in Table. 1.

Pulse Shape	6 th derivative Gaussian pulse
Pulse Width	0.168 ns
Pulse Amplitude	3 μ volts
Channel Model	S-V channel model (CM 3)
Transmission Multiple Access Techniques	<ul style="list-style-type: none"> • Direct Sequence • Time Hopping
Modulation Techniques	<ul style="list-style-type: none"> • Bi-phase Modulation (BPM) for DS • Pulse-Position-Modulation (PPM) for TH
PN Code Length	$N_c = 16$
Interferences	<ul style="list-style-type: none"> • NBI from IEEE 802.11a WLAN • MUI from 15 UWB users
Receiver Schemes	<ul style="list-style-type: none"> • Rake Receiver • MMSE Correlator with LMS, RLS adaptive algorithms
Chip Rate	1.6 GHz

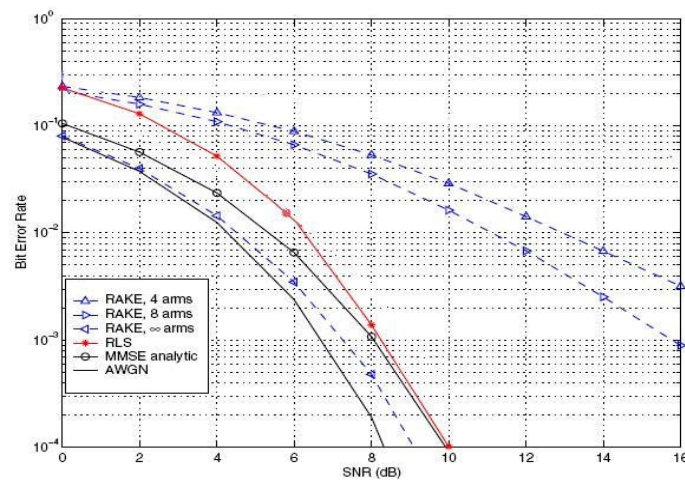


Fig. 11: Performance of DS-UWB over Multipath NLOS Channel with AWGN but no Interference

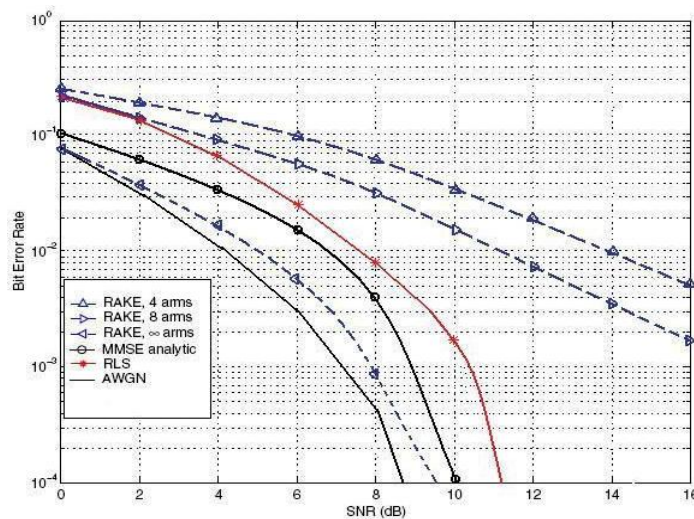


Fig. 12: Performance of TH-UWB over Multipath NLOS Channel with AWGN but no Interference

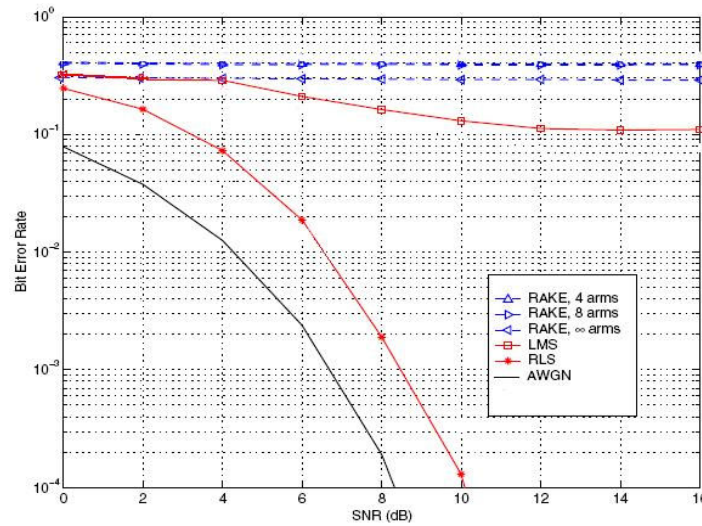


Fig. 13: Performance of DS-UWB over Multipath NLOS Channel with One NBI (SIR= -30 dB)

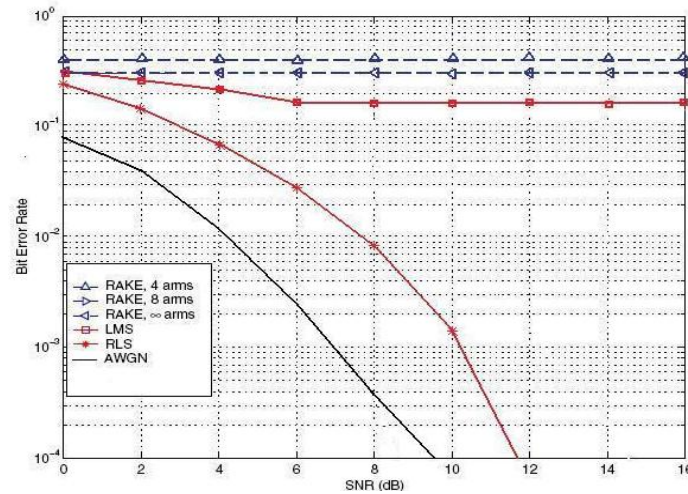


Fig. 14: Performance of TH-UWB over Multipath NLOS Channel with One NBI (SIR= -30 dB)

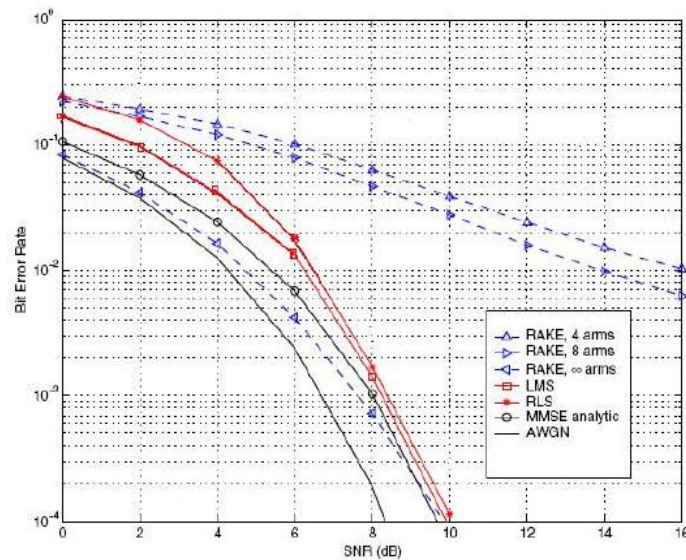


Fig. 15: Performance of DS-UWB over Multipath NLOS Channel with One Stronger NBI (SIR= 0 dB)

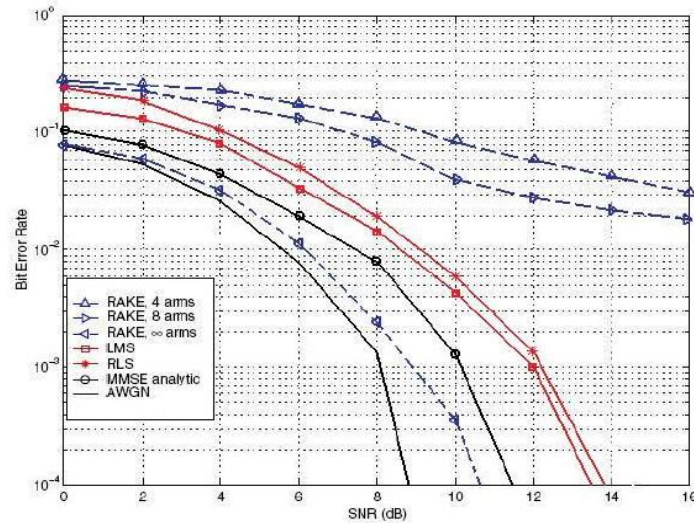


Fig. 16: Performance of TH-UWB over Multipath NLOS Channel with One Stronger NBI (SIR= 0 dB)

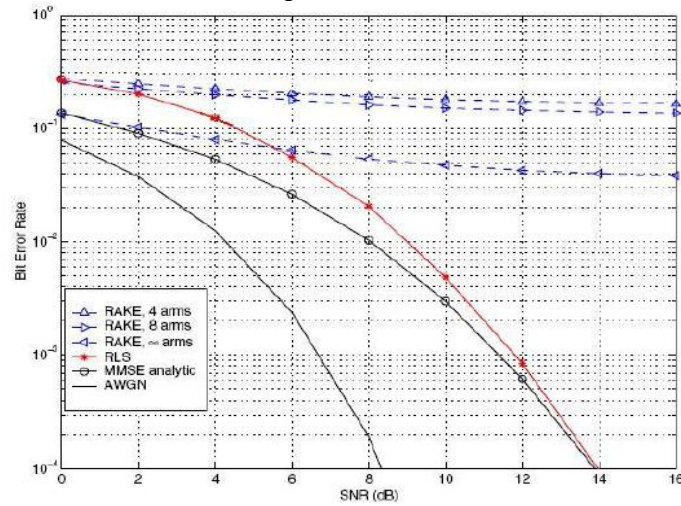


Fig. 17: Performance of DS-UWB over Multipath NLOS Channel with Multiple UWB Interferers (MUI of 15 UWB users)

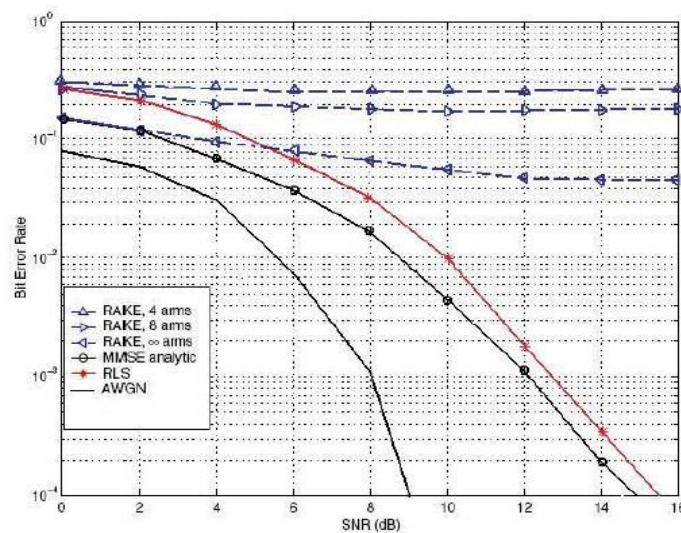


Fig. 18: Performance of TH-UWB over Multipath NLOS Channel with Multiple UWB Interferers (MUI of 15 UWB users)

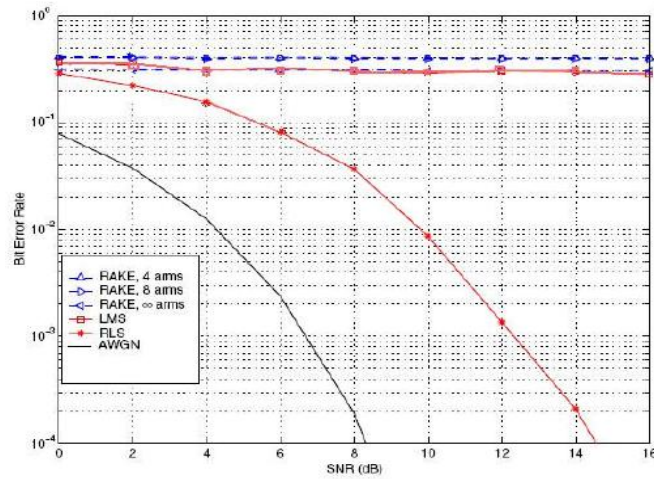


Fig. 19: Performance of DS-UWB over Multipath NLOS Channel with combined NBI (SIR = -30 dB) and Multiple UWB Interferers (MUI)

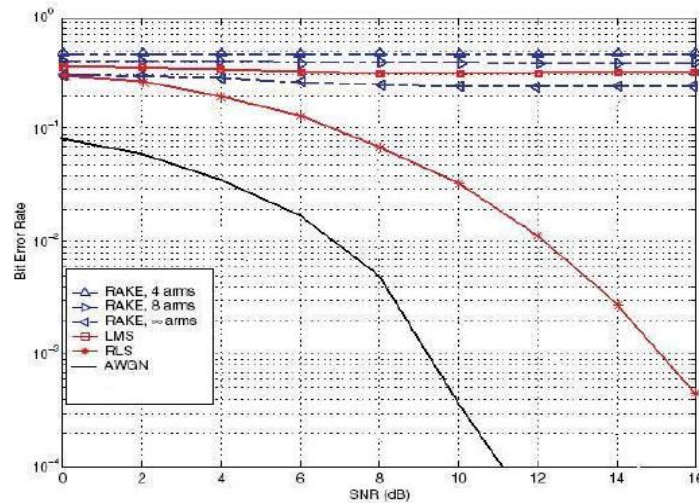


Fig. 20: Performance of TH-UWB over Multipath NLOS Channel with combined NBI (SIR = -30 dB) and Multiple UWB Interferers (MUI)

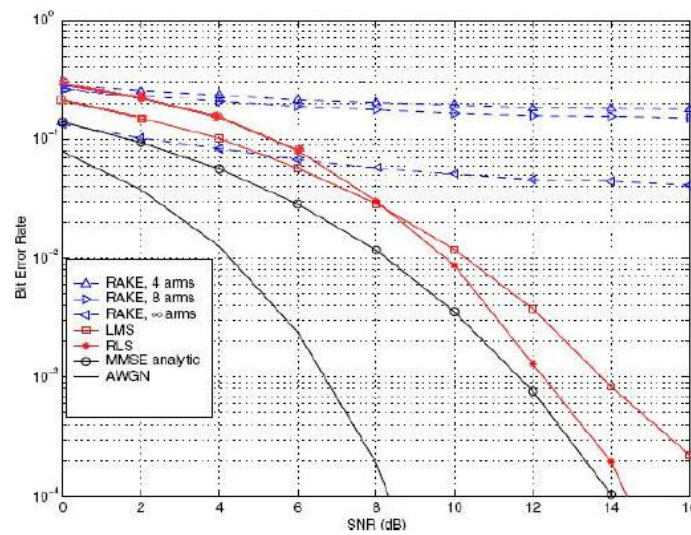


Fig. 21: Performance of DS-UWB over Multipath NLOS Channel with combined Stronger NBI (SIR = 0 dB) and Multiple UWB Interferers (MUI)

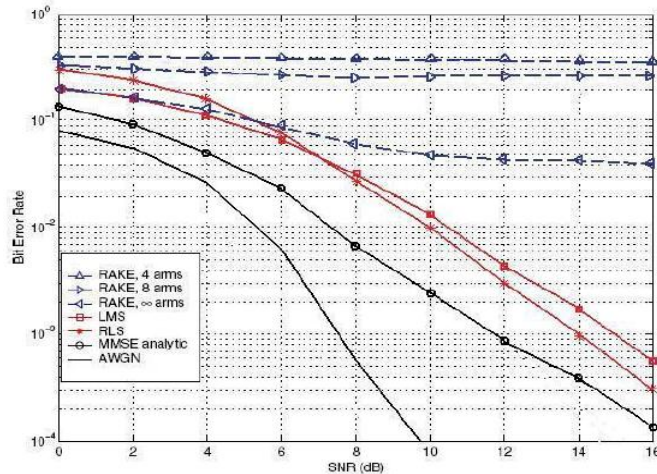


Fig. 22: Performance of TH-UWB over Multipath NLOS Channel with combined Stronger NBI (SIR = 0 dB) and Multiple UWB Interferers (MUI)

Furthermore, as demonstrated in the previous MATLAB simulation Figures (11, 12, 13... 22); the paper has examined the performance of both; Rake receiver structure with different number of Rake fingers, and MMSE correlator receiver structure analytically and with different adaptive algorithms RLS and LMS using the simulation key parameters in Table. 1 for the following five scenarios:

- Multipath NLOS Channel with only AWGN but no Interference (neither NBI nor MUI).
- Multipath NLOS Channel with the effect of a single NBI Source with SIR= -30 dB
- Multipath NLOS Channel with the effect of a stronger single NBI Source with SIR= 0 dB
- Multipath NLOS Channel with the effect of Multiple UWB Interference sources (15 MUI sources).
- Multipath NLOS Channel with the combined effect of both single NBI source and Multiple UWB Interference sources (15 MUI sources).

VI. CONCLUSION

This paper presents a detailed performance evaluation of two significant UWB reception structures and schemes; UWB Rake receiver with different number of Rake fingers (4, 8, and 128 “infinite”), and MMSE correlator receiver with different adaptive algorithms (RLS, and LMS), using the 6th derivative Gaussian pulse a new template UWB pulse over multipath NLOS channel based on the modified (S-V) channel model CM3 utilizing DS and TH as transmission and multiple access techniques. Based on the simulation key parameters in Table (1) examined for the five study case scenarios stated in the previous section, the simulation results show that; performance of DS-UWB as a transmission and multiple access technique is slightly better than TH-UWB technique specially in the presence of either Narrowband Interference (NBI) or Multiple User Interference (MUI) in addition to the AWGN. Furthermore, as the Narrowband Interference grow stronger (poorer SIR); the performance of Rake receiver with more Rake fingers is proven to be more efficient than the one with less Rake fingers. However, the reception performance has obviously improved and extensively developed when employing the Minimum Mean Square Error (MMSE) correlator receiver whether analytically or utilizing adaptive filter algorithms such as RLS and LMS specially in case of MUI caused by other UWB users in the proximity of the main desired UWB source.

VII. ACKNOWLEDGEMENT

In this section I would like to express my deepest gratitude to Jazan University represented by Deanship of Community Service and Continuing Education for the great support and facilitating all the required resources for this research to be accomplished.

REFERENCES

- [1] Ian Oppermann, Matti Hamalainen “UWB Theory and Applications,” Book, pp. 15–80.
- [2] M.Ghavami, L.B.Michael “Ultra-Wideband Signals and Systems in Communication Engineering,” Book, pp. 26–113.
- [3] B. M.Mezzour, “Direct Sequence UWB performance over STDL ” paper Journal, vol.3.

- [4] Nadir. Abd Elaziz, Abdelrasoul. Alzubaidi, "Performance of the 6th derivative Gaussian Pulse Shape in IEEE 802.15.3a Multipath Fading Channel" *IOSR journal of Engineering*, Vol3, Issue December 2014.
- [5] Rashid A. Fayyadh, F. Malik "Adaptive Rake receiver using Matched Filter with Three Combining Techniques" *Australian Journal of Basic and Applied Sciences*, 7(5): 26-33, 2013 ISSN 1991-8178.
- [6] Rashid A. Fayyadh, "Improved Rake Receiver Based On the Signal Sign Separation in Maximal Ratio Combining Technique for Ultra-Wideband Wireless Communication" *World Academy of Science, Engineering and Technology, International Journal of Electrical, Robotics, Electronics and Communications Engineering* Vol:7 No:12, 2013

BIOGRAPHY



Nadir Mohamed Abdelaziz, an Assist. Professor in Jazan University – CNET Dept.- Deanship of Community Service and Continuing Education, granted his B.SC and his M.SC degrees in Electronics and Communications Engineering from Arab Academy for Science & Technology (AAST)-Alexandria-Egypt, and his Ph.D degree in Communications Engineering from Al Neelain University – Khartoum-Sudan.